AMERICAN SOCIETY FOR MICROBIOLOGY | Journal of Bacteriology®

RESEARCH ARTICLE

The Phosphatidyl-*myo*-Inositol Dimannoside Acyltransferase PatA Is Essential for *Mycobacterium tuberculosis* Growth *In Vitro* and *In Vivo*

Francesca Boldrin,[a] Itxaso Anso,[b] Sogol Alebouyeh,[c] Iker A. Sevilla,[d] Mariví Geijo,[d] Joseba M. Garrido,[d] Alberto Marina,[b] Laura Cioetto Mazzabò,[a] Greta Segafreddo,[a] Marcelo E. Guerin,[b,e] Riccardo Manganelli,[a] Rafael Prados-Rosales[c]

[a]Department of Molecular Medicine, University of Padova, Padua, Italy
[b]Center for Cooperative Research in Biosciences (CIC bioGUNE), Basque Research and Technology Alliance (BRTA), Derio, Spain
[c]Department of Preventive Medicine and Public Health and Microbiology, Autonoma University of Madrid, Madrid, Spain
[d]Animal Health Department, NEIKER-Instituto Vasco de Investigación y Desarrollo Agrario, Derio, Spain
[e]IKERBASQUE, Basque Foundation for Science, Bilbao, Spain

ABSTRACT *Mycobacterium tuberculosis* comprises an unusual cell envelope dominated by unique lipids and glycans that provides a permeability barrier against hydrophilic drugs and is central for its survival and virulence. Phosphatidyl-*myo*-inositol mannosides (PIMs) are glycolipids considered to be not only key structural components of the cell envelope but also the precursors of lipomannan (LM) and lipoarabinomannan (LAM), important lipoglycans implicated in host-pathogen interactions. Here, we focus on PatA, a membrane-associated acyltransferase that transfers a palmitoyl moiety from palmitoyl coenzyme A (palmitoyl-CoA) to the 6-position of the mannose ring linked to the 2-position of inositol in PIM_1/PIM_2. We validate that the function of PatA is vital for *M. tuberculosis in vitro* and *in vivo*. We constructed a *patA* conditional mutant and showed that silencing *patA* is bactericidal in batch cultures. This phenotype was associated with significantly reduced levels of Ac_1PIM_2, an important structural component of the mycobacterial inner membrane. The requirement of PatA for viability was also demonstrated during macrophage infection and in a mouse model of infection, where a dramatic decrease in viable counts was observed upon silencing of the *patA* gene. This is reminiscent of the behavior of PimA, the mannosyltransferase that initiates the PIM pathway, also found to be essential for *M. tuberculosis* growth *in vitro* and *in vivo*. Altogether, the experimental data highlight the significance of the early steps of the PIM biosynthetic pathway for *M. tuberculosis* physiology and reveal that PatA is a novel target for drug discovery programs against this major human pathogen.

IMPORTANCE Tuberculosis (TB) is the leading cause of death from a single infectious agent. The emergence of drug resistance in strains of *M. tuberculosis*, the etiologic agent of TB, emphasizes the need to identify new targets and antimicrobial agents. The mycobacterial cell envelope is a major factor in this intrinsic drug resistance. Here, we have focused on the biosynthesis of PIMs, key virulence factors and important components of the cell envelope. Specifically, we have determined that PatA, the acyltransferase responsible for the first acylation step of the PIM synthesis pathway, is essential in *M. tuberculosis*. These results highlight the importance of early steps of the PIM biosynthetic pathway for mycobacterial physiology and the suitability of PatA as a potential new drug target.

KEYWORDS tuberculosis, *Mycobacterium tuberculosis*, conditional mutant, acyltransferase, glycolipid, mycobacterium

Mycobacterium tuberculosis, the etiologic agent of tuberculosis (TB), is the second most deadly infectious agent in the world after HIV. In 2018, there were about 10 million new cases and 1.2 million deaths from TB, with an estimated one-quarter of

Citation Boldrin F, Anso I, Alebouyeh S, Sevilla IA, Geijo M, Garrido JM, Marina A, Mazzabò LC, Segafreddo G, Guerin ME, Manganelli R, Prados-Rosales R. 2021. The phosphatidyl-*myo*-inositol dimannoside acyltransferase PatA is essential for *Mycobacterium tuberculosis* growth *in vitro* and *in vivo*. J Bacteriol 203:e00439-20. https://doi.org/10.1128/JB.00439-20.

Editor Laurie E. Comstock, Brigham and Women's Hospital/Harvard Medical School

Address correspondence to Riccardo Manganelli, riccardo.manganelli@unipd.it, or Rafael Prados-Rosales, rafael.prados@uam.es.

Received 30 July 2020
Accepted 30 December 2020
Accepted manuscript posted online 19 January 2021
Published 8 March 2021

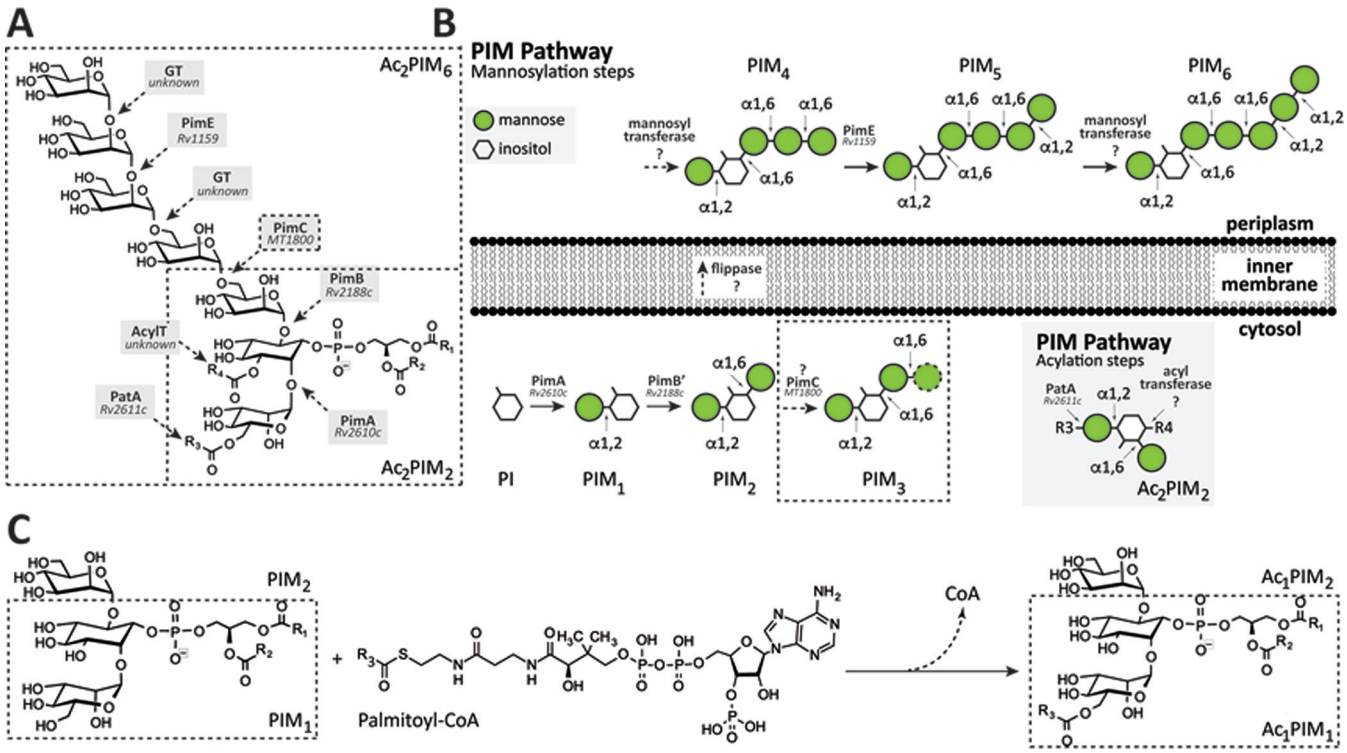

FIG 1 The PIMs from *M. tuberculosis*. (A) The chemical structure of PIMs. The major PIM species have two (PIM_2) or six (PIM_6) mannose residues with different degrees of acylation. (B) The current model of PIM biosynthesis. The currently accepted model proposes that PimA and PimB catalyze the two first consecutive mannosylation steps in the cytoplasmic face of the plasma membrane. The identity and location of the enzyme(s) responsible for the third and fourth mannosylation steps, as well as the existence of a flippase, are under debate. The fifth mannosylation step is catalyzed by PimE in the periplasmic face of the plasma membrane. The identity of the enzyme responsible for the sixth mannosylation step is still unknown. PIMs can be also acylated by the action of two acyltransferases: PatA catalyzes the transfer of an acyl chain to the mannose ring transferred by PimA at the cytosolic face of the plasma membrane, whereas an unknown acyltransferase catalyzes the transfer of an acyl chain to the inositol ring of the glycolipid. In the inset, the acylation steps on Ac_2PIM_2 are shown as an example. (C) PatA transfers a palmitoyl moiety from palmitoyl-CoA to the 6-position of the mannose ring linked to 2-position of inositol in PIM_1/PIM_2.

the human population carrying a latent infection (1–4). First-line treatment for active, drug-susceptible TB, requires a standard administration of four drugs during a period of 6 months, including isoniazid, rifampicin, ethambutol, and pyrazinamide (5). Multidrug-resistant TB (MDR-TB) and extensively drug-resistant TB (XDR-TB) emerge mainly as a result of poor compliance during short-course chemotherapy (6). Specifically, MDR-TB is a form of TB caused by bacteria that do not respond to isoniazid and rifampicin. Although MDR-TB is curable, it requires expensive and toxic second-line drugs and an extensive chemotherapy of up to 2 years. XDR-TB is a more serious form of MDR-TB caused by bacteria that do not respond to the most effective second-line anti-TB drugs, often leaving patients without any further treatment options (6). MDR-TB and XDR-TB remain a public health crisis and a health security threat, making the discovery of new targets and novel anti-TB drugs with bactericidal mechanisms different from those of currently available agents an urgent need (7). The cell envelope of *M. tuberculosis* exhibits a unique architecture comprised of sugars and lipids of exceptional chemical structure, providing a hydrophobic impermeable barrier against many commonly used antibiotics and allowing the bacteria to survive in extremely hostile intracellular conditions. Due to its essential role in the biology of *M. tuberculosis*, the cell envelope represents a highly attractive target for the discovery of novel anti-TB drugs (8–10). In that sense, several key medicines used in current TB therapy inhibit enzymes involved in cell envelope biosynthesis.

The phosphatidyl-*myo*-inositol mannosides (PIMs) are glycolipids found in abundant quantities in the inner and outer membranes of the cell envelope of *Mycobacterium* spp. and a few other actinomycetes (Fig. 1) (11–13). PIMs are based on a phosphatidyl-*myo*-inositol (PI) anchor and can contain one to six mannose residues and up to four acyl chains.

The tri- and tetra-acylated phosphatidyl-*myo*-inositol dimannosides (Ac_1PIM_2 and Ac_2PIM_2, respectively) are considered both metabolic end products and intermediates in the biosynthesis of the tri- and tetra-phosphatidyl-*myo*-inositol hexamannosides (Ac_1PIM_6 and Ac_2PIM_6, respectively), lipomannan (LM), and lipoarabinomannan (LAM) (11, 12, 14). PIMs, LM, and LAM play an essential role as structural components of the mycobacterial cell envelope but are also important molecules implicated in host-pathogen interactions in the course of TB and leprosy (11, 13, 15–18). The biosynthesis of PIMs takes place on both sides of the mycobacteria inner membrane (Fig. 1) (12, 13). The biosynthesis of PIMs is initiated on the cytoplasmic side by the mannosyltransferase PimA (Rv2610c; the Rv numbers of the nomenclature based on the *M. tuberculosis* H37Rv genome are included hereafter), which catalyzes the transfer of a mannose residue from GDP-mannose (GDP-Man) to the 2-position of the *myo*-inositol ring of PI to produce phosphatidyl-*myo*-inositol monomannoside (PIM_1 [19, 20]). The second step is mediated by the mannosyltransferase PimB (Rv2188c), which transfers a mannose residue from GDP-Man to the 6-position of the *myo*-inositol ring of PIM_1, to produce phosphatidyl-*myo*-inositol dimannoside (20–23). The acyltransferase PatA catalyzes the transfer of a palmitoyl moiety from palmitoyl coenzyme A (palmitoyl-CoA) to PIM_1 and PIM_2 at the 6-position of the mannose ring transferred by PimA to form Ac_1PIM_1 and Ac_1PIM_2, respectively (24–26). The following two pathways were originally proposed for the biosynthesis of Ac_1PIM_2: (i) PI is mannosylated by the consecutive action of PimA and PimB to form PIM_2, which is further acylated to form Ac_1PIM_2, and (ii) PIM_1 is acylated by PatA to form Ac_1PIM_1 and then mannosylated by PimB to form Ac_1PIM_2. The experimental data indicate that both pathways might coexist in mycobacteria, although the sequence of events PI→PIM_1→PIM_2→Ac_1PIM_2 is favored (20, 27, 28). Ac_1PIM_2 can be further acylated on position 3 of the *myo*-inositol ring to form Ac_2PIM_2 (20, 28). This acyltransferase as well as most of the mannosyltransferases involved in the biosynthesis of higher forms of PIMs still remains to be identified (11–13, 29). Strikingly, the following four enzymes participating in the early steps of the PIM pathway were found to be essential *in vitro* in *Mycobacterium smegmatis*: the phosphatidylinositol phosphate synthase PIP (Rv2612c), PimA, PimB, and PatA (19, 26, 30, 31). From a drug discovery perspective, the essential character of the enzymes involved in the early steps of PIM biosynthesis and their restriction to mycobacteria and a few other actinomycetes highlight their interest as novel targets for TB drug discovery (12, 13).

Here, we focus on PatA (2.3.1.265), an enzyme that belongs to an important family of acyltransferases, including HtrB and MsbB, involved in the last steps of Kdo2-lipid A biosynthesis in Gram-negative bacteria (32). We previously provided the very first crystal structures of PatA in the presence of (i) its naturally occurring acyl donor palmitoyl group, (ii) a nonhydrolyzable palmitoyl-CoA analog, and (iii) the 6-*O*-palmitoyl-α-D-mannopyranoside product, unraveling the acyl donor and acceptor binding mechanisms (32, 33). In this study, we carefully investigated the essentiality of PatA from *M. tuberculosis in vitro* and *in vivo*, in a mouse model of TB, in order to evaluate its potential for drug discovery purposes.

RESULTS

Silencing of *patA* in axenic cultures results in bacterial death. To probe the essentiality of PatA, a conditional knockdown (cKD) mutant for the *patA* gene (*rv2611c*) (TB489) was constructed in *M. tuberculosis* H37Rv as described in Materials and Methods. Since *patA* is part of a predicted operon including *pimA* (*rv2610c*) and *rv2609c* (19, 20, 34), to avoid artifacts due to polar effects, both genes were provided in *trans* on pFRA247, a pMV261-derived plasmid expressing the two genes from the constitutive promoter P_{hsp60}. In the resulting strain, named TB506.1, expression of *patA* was expected to be downregulated following the addition of anhydrotetracycline (ATc) to the culture medium.

As shown in Fig. 2A, when serial dilutions of a TB506.1 suspension were spotted on Middlebrook 7H10 containing 500 ng/ml ATc, bacterial growth was inhibited, confirming the predicted essentiality of *patA in vitro*. The visible residual growth corresponds

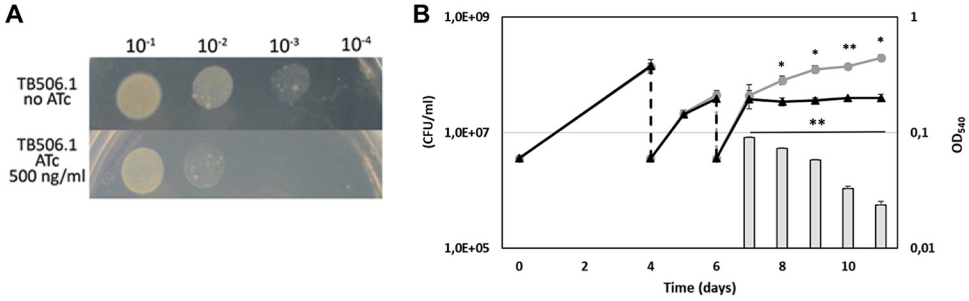

FIG 2 *patA* is an essential gene in *M. tuberculosis*. (A) Serial dilutions of log-phase cultures of the conditional mutant TB506.1 were spotted on Middlebrook 7H10 plates with or without 500 ng/ml ATc. (B) Growth curves of the conditional knockdown TB506.1 in the presence (triangles) or absence (circles) of 500 ng/ml ATc; 1:10 dilutions of the cultures in fresh medium with or without ATc (dashed arrows) were performed until the growth of the culture with ATc stopped. Gray bars represent the number of CFU per milliliter in the culture with ATc after its growth arrested. The results represent the average of three independent experiments. *, $P < 0.5$; **, $P < 0.05$.

to spots containing the largest number of bacteria, suggesting that bacteria must go through some generations before PatA is titrated down and the phenotype becomes detectable. As expected, the growth of TB38, an *M. tuberculosis* H37Rv derivative containing pFRA61 (carrying the TetR/PipOFF) on the chromosome, was unaffected by the presence of the drug at this concentration (see Fig. S2 in the supplemental material). A similar experiment was performed growing the bacteria in Middlebrook 7H9 liquid medium with or without ATc (500 ng/ml). As depicted in Fig. 2B, two passages in fresh ATc-containing medium were necessary to observe bacterial growth inhibition, confirming that some time was necessary to titrate down PatA after the downregulation of its structural gene. We also followed the viability of the culture of the *patA* conditional mutant grown in the presence of ATc after its growth curve diverged from that of the culture grown without ATc. As visible in Fig. 2B, despite the optical density of the culture with ATc remaining stable, the number of viable cells decreased, suggesting that PatA depletion is bactericidal.

To demonstrate that the observed phenotype was indeed due to the downregulation of *patA* and not to the failure to complement *pimA* (*rv2609c*) with pFRA247, this plasmid was transformed in a previously characterized *pimA* (*rv2609c*) conditional mutant TB99 (34) to obtain TB513. In this case, pFRA247 was able to complement the downregulation of *pimA*, as the presence of ATc did not affect the growth of this complemented strain (see Fig. S3 in the supplemental material). Further, to confirm expression of *pimA* in the *patA* mutant, we performed a side-by-side reverse transcriptase PCR (RT-PCR) analysis of both *pimA* and *patA* in TB99 and TB506.1 strains. We found that levels of *pimA* expression were comparable in the two strains in the absence of ATc, while in the presence of ATc, *pimA* was exclusively repressed in TB99 and *patA* was exclusively repressed in TB506.1 (see Fig. S4 in the supplemental material). Importantly, it is worth noting that the mRNA levels of *rv2612c* remained constant in strains TB99 and TB506.1 (Fig. S4).

Production of PIM is greatly reduced in *patA*-depleted mycobacteria. The effect of *patA* gene silencing on PIM biosynthesis was examined by one-dimensional and two-dimensional (2D) thin-layer chromatography (TLC) analysis of the lipids extracted from *M. tuberculosis* TB38 and TB506.1 cells collected at different time points (0, 4, and 12 days) in medium supplemented with 500 ng/ml ATc. Lipid identification was performed by calculating the retention factor (R_f) value, defined as the distance travelled by a given compound divided by the distance traveled by the solvent (35), and comparing to previous reports using the same experimental setup. As expected, the TB38 strain showed a similar lipid profile during the time course (Fig. 3A). In contrast in the TB506.1 strain, we could observe a reduction in lipid bands I, II, and III, starting from the origin (O), corresponding to Ac_1PIM_6, Ac_2PIM_6, and Ac_1PIM_2, respectively (Fig. 3A)

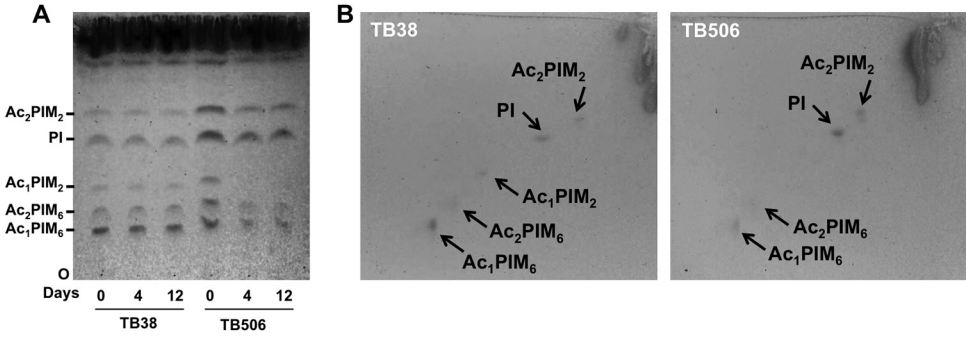

FIG 3 Loss of Ac_1PIM_2 in the PatA-depleted strain. (A) Lipids were extracted from *M. tuberculosis* TB38 and TB506.1 grown in the presence of 500 ng ml^{-1} ATc at different time points (0, 4, and 12 days), separated by TLC in the solvent $CHCl_3$-CH_3OH-concentrated NH_4OH-H_2O (65:25:0.5:4) and visualized with α-naphthol. (B) Alternatively, samples from day 12 were separated by 2D-TLC using the same solvent system as in panel A for dimension 1 and chloroform, acetic acid, methanol, and water (50:60:2.3:3) for dimension 2 and visualized as in panel A. Data are representative of two independent experiments with similar results. At the indicated days, cultures were submitted to serial dilutions in fresh medium with ATc in order to visualize a progressive decrease in the Ac_1PIM_2 levels.

(19), and an increase in the lipid band assigned to PI relative to the TB38 strain (Fig. 3A) (36).

We performed 2D-TLC analysis of the same samples and corroborated that production of Ac_1PIM_6, Ac_2PIM_6, and Ac_1PIM_2 lipid species is affected in the TB506.1 strain relative to the TB38 strain (Fig. 3B). This was particularly evident in the case of Ac_1PIM_2, which is absent in the mutant and is considered an end product of the PIM pathway (12, 13, 18). Altogether, this profile is consistent with the biochemical reaction catalyzed by PatA, which transfers a palmitoyl moiety from palmitoyl-CoA to the 6 position of the mannose ring linked to the 2 position of *myo*-inositol in PIM_1 or PIM_2, leading to the synthesis of Ac_1PIM_1/Ac_1PIM_2. It is evident that depletion of PatA caused a block in the biosynthesis of PIMs, resulting in severe changes in the composition of the mycobacterial cell membrane, which correlates with the loss of viability observed.

***patA* is essential for growth in macrophages.** To validate the essentiality of *patA* during intracellular growth on macrophages, we infected THP-1-derived macrophages with the *patA* conditional mutant TB506.1 and the parental strain TB38, in the presence or absence or ATc, and determined viable counts 2, 4, and 6 days after infection. Both TB38 parental strain and TB506.1 retained their infective capacity in the absence of ATc and beside the presence of TetR and Pip regulators. Conversely, only the TB506.1 strain showed reduced viability on the presence of ATc being significantly reduced at day 4 and 6 after infection (Fig. 4). Importantly, no difference in cell viability was observed between treatments (data not shown). These results indicate the essentiality of *patA* for macrophage infection.

***patA* is essential for growth in mouse.** To assess the essentiality of *patA in vivo*, C57BL/6J mice were intranasally infected with the conditional mutant strain TB506.1. Silencing of *patA* was achieved by supplying animals with water with 5% sucrose containing doxycycline starting on the day of the infection. Control groups did not received doxycycline, allowing normal expression of *patA*. As depicted in Fig. 5, we observed that *M. tuberculosis* H37Rv sustained infection in the presence and in the absence of doxycycline, 4 and 8 weeks after challenge. In the same line, the TB506.1 mutant in the absence of doxycycline reached similar rates of bacterial replication during the acute (4 weeks) and chronic (8 weeks) phases of infection. In contrast, TB506.1 manifested a dramatic reduction in CFU at 4 and 8 weeks after infection in the presence of doxycycline, indicating the essential nature of *patA* during both the acute and chronic phases of infection. This significant trend of reduction in cell viability for TB506.1 in the presence of doxycycline was observed in both lungs and spleen. Altogether, these findings clearly highlight the essential role played by PatA during *M. tuberculosis* infection.

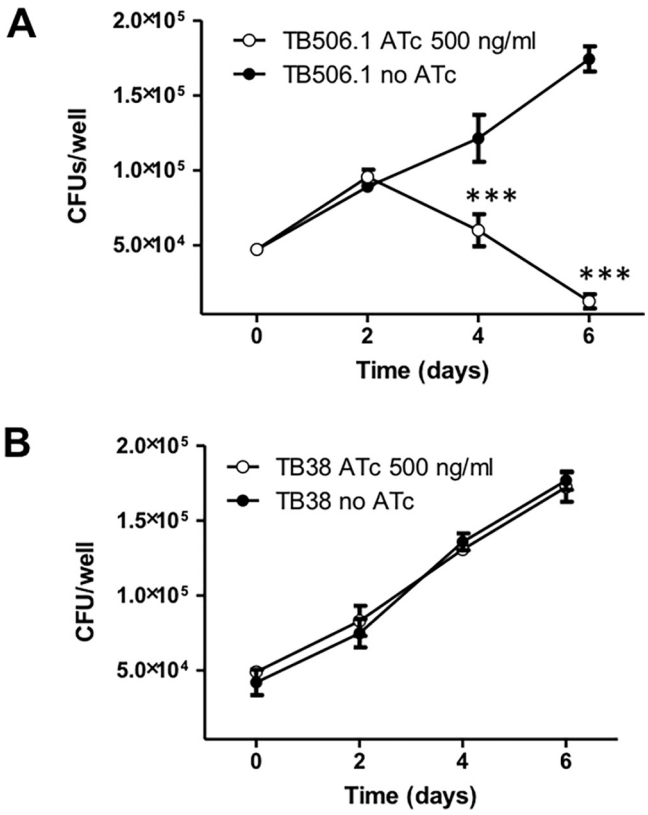

FIG 4 Growth curves of TB506.1 and of the parental strain TB38 in THP-1-derived macrophages. The *patA* conditional mutant TB506.1 and the parental strain TB38 were used to infect THP-1-derived macrophages. While TB506.1 was able to replicate intracellularly only in the absence of ATc (A), TB38 was able to divide regardless of the presence of ATc in the cell culture medium (B). Filled circles, no ATc; open circles, 500 ng/ml ATc added to the culture medium. Data are representative of two independent experiments with similar results. ***, $P < 0.001$ one-way ANOVA with Tukey posttest.

DISCUSSION

The gene *patA* is predicted to be an essential gene for *in vitro* growth of H37Rv according to analysis of saturated Himar1 transposon libraries (31, 37, 38). The aim of this work is to demonstrate the essentiality of *patA* during *in vitro* growth and experimental macrophage and mouse infections. These results strongly suggest that the membrane acyltransferase PatA is a potential drug target in *M. tuberculosis* according to its essentiality.

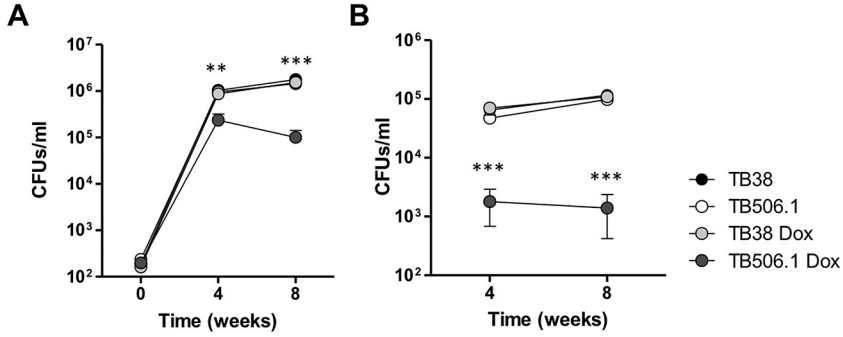

FIG 5 Validation of *patA* essentiality in the mouse model of infection. The graph illustrates the bacterial loads in the lungs (A) and spleens (B) of C57BL/6JOlaHsd mice infected with TB506.1. Silencing of *patA* was achieved by supplying animals with water supplemented with 5% sucrose containing doxycycline. Results represent the mean value and error for 5 mice per group and time point. **, $P < 0.01$; ***, $P < 0.001$ one-way ANOVA with Tukey posttest.

We did this by exploiting a repressible promoter system based on the TetR and Pip regulators (34, 39). The *patA* gene is part of a cluster of genes potentially organized as a single transcriptional unit (12, 26) involved in the early steps of PIM biosynthesis. The upstream gene encodes the phosphatidylinositol phosphate synthase PIP (Rv2612c) (*rv2612c*, *PIP*) (30, 40–42), whereas the downstream open reading frame (ORF) encodes a putative GDP-mannose hydrolase (*rv2609c*) and the phosphatidyl-*myo*-inositol mannosyltransferase PimA (*rv2610c*) (19, 20). Although *rv2609c* was predicted to be nonessential (37), we decided to provide this ORF and that of the *pimA* gene in *trans* on a replicative plasmid to the TB506.1 strain in order to counteract potential polar effects caused by the single recombination event in the *patA* gene. In this regard, we are confident that the described phenotype is therefore due to the lack of the *patA* gene product only.

When grown on solid medium, the conditional mutant was clearly able to replicate only in the absence of ATc, and the same phenotype was evident also in liquid medium. Moreover, to observe an effect during growth in liquid culture, cells had to undergo two passages. This suggests that the conditional mutant accumulation of both PatA and PIMs allows cell growth for several rounds of replication after *patA* expression is repressed. This phenomenon has already been observed for other conditional mutants generated using the same TetR/PipOFF system and could be due to the higher strength of the *ptr* promoter compared to that of the original promoter of the downregulated gene causing its overexpression in the absence of ATc (43, 44). The sharp decrease of bacterial viability following *patA* repression resembled that observed after repression of *pimA* and expanded the essentiality to the early steps of the PIM biosynthetic pathway (12, 18). Biochemical analyses of the lipids after *patA* repression showed a clear depletion of PIMs and a consequent accumulation of the PIMs precursor PI, with no effect on the remaining pools of lipids, further supporting the essential role of PatA in this biochemical pathway.

The observed accumulation of PI and depletion of PIMs in the TB506.1 strain upon treatment with ATc seem to be deleterious during experimental infection of both macrophages and mice. We observed a rapid decline in viable counts 2 days after macrophage infection, indicating that alteration of the PIM biosynthesis pathway is critical during the initial stages of infection. Although macrophages represent a starting point at the time of interrogating the role of *patA* during infection, our results suggest that *M. tuberculosis* needs to keep the integrity of the early steps of PIM biosynthesis for optimal intracellular replication. To test the role of this gene during a more relevant complex infection scenario, we infected C57BL/6 mice with TB506.1 and control strains and provided water supplemented with or without doxycycline. The dramatic and significant decrease in the number of CFU in lung and spleens both at 4 and 8 weeks after infection for the TB506.1 strain in the presence of doxycycline strongly supports that the absence of *patA* leads to loss of bacterial cell viability. Although we do not know the exact mechanism by which silencing of *patA* might have accelerated the process of lung clearance, it is possible that some cell envelope instability due to altered lipid composition renders *M. tuberculosis* more susceptible to innate and adaptive immune responses.

Ac_2PIM_2 was found to be the most abundant lipid group in the inner membrane (IM), accounting for up to 42% (by weight) of all of the lipids in the IM extract (16, 44–47). Our TLC analysis indicates the complete disappearance of Ac_1PIM_2 and the reduction of Ac_1PIM_6 and Ac_2PIM_6 glycolipid species in the TB506.1 strain relative to the TB38 strain (Fig. 3B). The accumulation of PI in the *M. tuberculosis patA*-deficient mutant is somehow expected as well as the accumulation of PIM_1 and/or PIM_2. Indeed, Kordulakova and colleagues have demonstrated the accumulation of PIM_1 and PIM_2 glycolipids in an *M. smegmatis patA*-deficient mutant (26). The lack of the palmitoyl residue in Ac_2PIM_2 glycolipid can certainly modify the properties of the mycobacterial cell envelope (48). In that sense, the *M. smegmatis patA* mutant could only be grown in the presence of a high concentration of NaCl (15 g/liter) and in the absence of Tween 80. The sodium salts might protect the weakened membrane by osmotic pressure or by

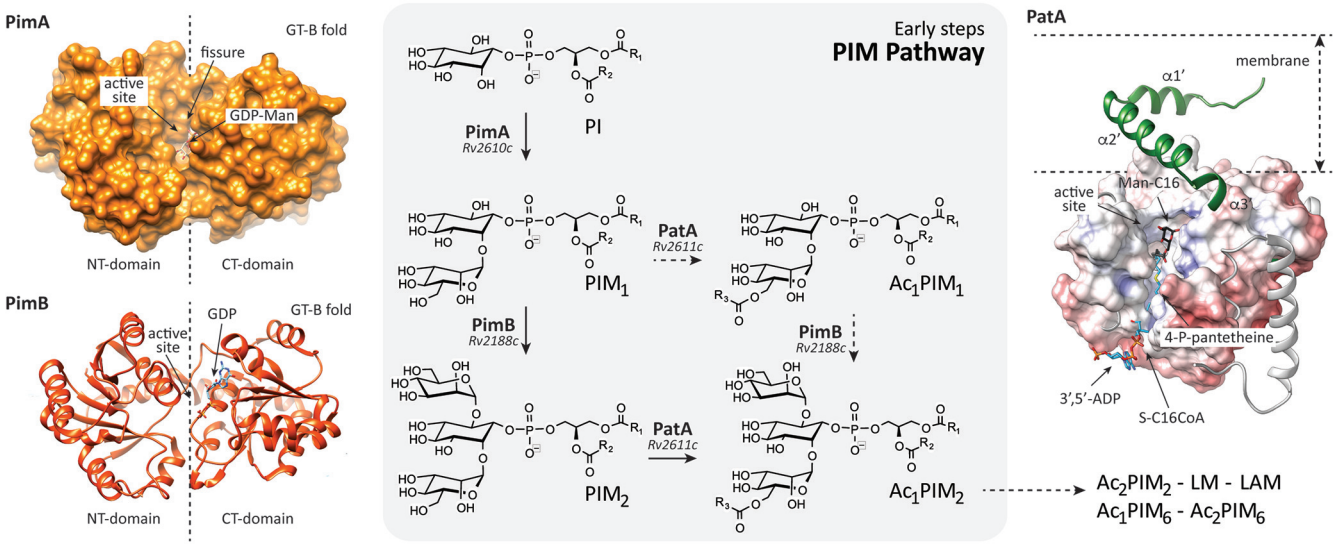

FIG 6 Essentiality of the early steps in PIM biosynthesis. Two pathways were originally proposed for the biosynthesis of Ac_1PIM_2 in the cytoplasmic phase of the mycobacterial inner membrane as follows: (i) PI is mannosylated to form PIM_2 by the consecutive action of the GT-B glycosyltransferases PimA and PimB, respectively, and PIM_2 is then acylated by PatA to form Ac_1PIM_2; and (ii) PI is mannosylated by PimA to form PIM_1 and then acylated by PatA to form Ac_1PIM_1, which in turn is mannosylated by PimB to form Ac_1PIM_2. *In vitro* experimental evidence indicates that although both pathways might coexist in mycobacteria, the sequence of events PI→PIM_1→PIM_2→Ac_1PIM_2 is favored (20, 28). The production and purification of high yields of PimA, PimB, and PatA, along with the determination of their three-dimensional structure, place us in an unprecedented position to initiate a drug discovery program focusing on those enzymes (32, 33, 51–53).

neutralizing the surface charges of the membrane. Importantly, the mRNA levels of *rv2612c* remained constant in the two strains, TB99 and TB506.1, ruling out any defect in the PI biosynthesis. What seems interesting is the fact that, together with the complete disappearance of Ac_1PIM_2 and the reduction of Ac_1PIM_6 and Ac_2PIM_6, the levels of Ac_2PIM_2 remain unchanged. According to Bansal-Mutalik and colleagues, Ac_2PIM_2 is the major component of the internal leaflet of the mycobacterial inner membrane (45). One possible explanation for these results is the presence of compensatory acyltransferase activities/specificities that could contribute to generate and maintain the Ac_2PIM_2 levels (26). Taken together, the experimental data suggest that Ac_1PIM_2 and Ac_2PIM_2 primarily play a structural role in the mycobacterial cell envelope (49). The alteration in the relative abundance of lipids/glycolipids leads to structural defects in the mycobacterial cell envelope, explaining the observed severe growth defects. Therefore, *patA* is another potential target whose depletion causes severe consequences in *M. tuberculosis* cell viability, similar to what has been reported for other mycobacterial genes (34, 50).

Our long-term goal is the discovery of novel anti-TB drugs targeting the early steps of PIM biosynthesis. From a drug discovery perspective, the essential character of PIM biosynthetic enzymes and their restriction to mycobacteria and a few other actinomycetes emphasizes their interest as novel targets for anti-TB chemotherapeutic agents (Fig. 6). The following four enzymes of the PIM pathway were found to be essential in *M. smegmatis* and/or *M. tuberculosis*: (i) *in vitro*, PIP (Rv2612c [30]), PimA (Rv2610c [19, 34]), PimB (Rv2188c [20]), and PatA (Rv2611c [26; this study]); and (ii) *in vivo* in *M. tuberculosis*, PimA (34) and PatA (this study). Interestingly, the crystal structures of PimA, PimB, and PatA have been reported (32, 33, 51–53). PimA and PimB belong to the GT-B family of glycosyltransferases, consisting of two Rossmann fold domains with a deep fissure at the interface that includes the catalytic center (54–58). As a consequence, the occurrence of an important interdomain movement has been well established in GT-B enzymes (27, 59). Specifically, PimA is an outstanding example of GT-B flexibility and intrinsic dynamic properties for the study of GT-B enzymes. The crystal structures of the unliganded form of PimA and that of the GDP-Man complex revealed the local reshuffling of secondary structure elements within the flexible segment (residues 118

to 163) in the N-terminal domain (52). Very recently, we identified four functionally relevant states of PimA that coexist in dynamic equilibrium in solution undergoing conformational exchange on timescales from milliseconds to seconds. Specifically, fold switching is a slow process, on the order of seconds, whereas domain motions occur simultaneously but are substantially faster, on the order of milliseconds (60). We hypothesize that such conformational flexibility has impaired identification of potent inhibitors against PimA using *in silico* and *in vitro* target-based drug screening approaches. In contrast, the crystal structures of PatA in the presence of (i) its naturally occurring acyl donor palmitoyl group, (ii) a nonhydrolyzable palmitoyl-CoA analog, and (iii) the 6-*O*-palmitoyl-α-D-mannopyranoside product revealed clear defined grooves that participate in the association of the substrates and products. We hypothesize that the presence of clear and deep pockets might facilitate the *in silico* and *in vitro* screenings for the discovery of potent inhibitors against the enzyme.

Taken together, these data clearly show the essentiality of PatA for *M. tuberculosis* growth and survival in axenic cultures and during macrophage or mouse infection, making it a potential candidate for *in vitro* target-based drug screening approaches. Finally, the modulation of PimA or PatA expression by the use of the conditional mutant could find application in target-based whole-cell screening assays for the identification of compounds targeting PimA or PatA or other cellular processes that are part of the same pathway.

MATERIALS AND METHODS

Bacterial strains and media. *M. tuberculosis* strain H37Rv was grown at 37°C in Middlebrook 7H9 or 7H10 (Difco) supplemented with 0.05% (vol/vol) Tween 80 (Sigma-Aldrich), 0.2% (vol/vol) glycerol (Sigma-Aldrich), and 10% ADN (2% glucose, 5% bovine serum albumin, 0.85% NaCl). For cloning procedures, *Escherichia coli* strain DH5α was grown in Luria-Bertani medium (LB). When required, hygromycin (Roche) was used at a final concentration of 50 μg/ml for *M. tuberculosis* and 150 μg/ml for *E. coli*. Streptomycin and kanamycin (Sigma-Aldrich) were used at a concentration of 20 μg/ml. Anhydrotetracycline (Sigma-Aldrich) was used at a concentration of 500 ng/ml.

Construction of the *M. tuberculosis patA* conditional mutant. The *patA* (*rv2611c*) conditional mutant was constructed in *M. tuberculosis* H37Rv using the TetR/PipOFF repressible promoter system (39, 43). In this system, the gene of interest is placed under the transcriptional control of the repressible promoter P_{ptr}; then, the gene encoding its repressor (Pip) is introduced in the chromosome together with the gene encoding the repressor TetR. Since the gene encoding Pip is transcribed from a TetR-dependent promoter, addition of anhydrotetracycline (ATc) to the culture medium leads to its induction and consequent repression of the gene of interest (39).

To place *patA* under P_{ptr} transcriptional control, we constructed a suicide plasmid cloning the first 620 bp of the *patA* gene (PCR amplified using primers RP1862bis, 5′-CCAATGCATATTGCCGGCCTTAAGGGCT-3′, and RP1889, 5′-AGGCCTCAGACCACTCGGTTGTTCCT-3′) downstream P_{ptr} in pFRA50 (39), conferring resistance to hygromycin. Ten micrograms of the resulting plasmid (pFRA238) was then introduced by electroporation into *M. tuberculosis* H37Rv, and transformants were selected on 7H10 plated containing hygromycin (see Fig. S1A in the supplemental material). The correct integration of the suicide plasmid by insertional duplication was confirmed by PCR, using an upper primer in the P_{ptr} region (RP1908, 5′-CGACCTGACCGCGGAGAAAT-3′) and a lower primer external to the homology region used for recombination (RP1909, 5′-CAGCAATGTGTGGGCAGCAA-3′) (Fig. S1B). The resulting strain (TB498) was finally electroporated with the integrative plasmid pFRA61.1, containing the TetR-PipOFF system, conferring resistance to streptomycin to obtain TB499. Since *patA* might be cotranscribed with its downstream genes *rv2609c* and *rv2610* (*pimA*), we decided to provide these genes in *trans* expressed from a constitutive promoter so that addition of ATc would lead to the repression of only *patA* transcription. For this purpose, *pimA* and *rv2609c* were amplified from the H37Rv genome using the primers RP1890, 5′-AGGCCTCTCGGATCGGCATGATTTGTC-3′, and RP1891, 5′-GTCGACCGACTTTTCTAAGCGGTCCA-3′, and then cloned downstream P_{hsp60} in the replicative plasmid pMV261, conferring resistance to kanamycin. The resulting plasmid, named pFRA247, was than introduced in the conditional mutant TB499 to obtain TB506.1 (Table 1).

Characterization of the *patA* conditional mutant. To characterize the growth curves of the bacterial strains, mid-log cultures were diluted up to a theoretical optical density at 540 nm (OD_{540}) of 0.06 in Middlebrook 7H9 albumin-dextrose-catalase (ADC) with or without 500 ng/ml ATc and incubated without shaking at 37°C. OD_{540} was recorded at different time points to obtain the growth curves. To characterize the growth of the bacterial strains on solid medium, 5 μl of 10-fold serial dilutions of a mid-log culture grown in Middlebrook 7H9 ADC was spotted on Middlebrook 7H10 plates with or without 500 ng/ml ATc. Plates were than incubated at 37°C until growth was visible.

Extraction of lipids from the *patA*-deficient *M. tuberculosis* mutant. *M. tuberculosis* TB506.1 was grown at 37°C in standing Middlebrook 7H9 supplemented with 500 ng/ml ATc. The bacteria were diluted every 120 h three times in fresh ATc-containing medium and collected before each dilution.

TABLE 1 *M. tuberculosis* strains used in this study

Strain name	Parental strain	Description	Reference or source
TB38	H37Rv	TetR/PipOFF system	39
TB498	H37Rv	P_{ptr}*patA_pimA_rv2609c*	This paper
TB499	TB498	P_{ptr}*patA_pimA_rv2609c*, TetR/PipOFF system	This paper
TB506.1	TB499	TB499(pFRA247) (pMV261-derived plasmid expressing *pimA_rv2609c* under P_{hsp60})	This paper
TB99	H37Rv	P_{ptr}*pimA_rv2609c*, TetR/PipOFF system	34
TB513	TB99	TB99(pFRA247)	This paper

Cells were harvested by centrifugation at 3,500 rpm for 5 min, and pellets were heat inactivated at 100°C for 1 h and used for lipid extraction. A culture of *M. tuberculosis* TB506.1 grown without ATc served as a control. Five milliliters 2:1 (vol/vol) chloroform-methanol was added to the cell pellet and incubated at room temperature (RT) for 12 h with constant stirring. The organic extract was separated by centrifugation (1,000 × *g*, 5 min, RT) and decantation. The obtained pellet was extracted with 5 ml 2:1 (vol/vol) chloroform-methanol for 1 h at RT with constant stirring and separated under the same conditions. The combined two organic extracts were dried under a stream of nitrogen gas at RT and subjected to a biphasic Folch wash with 2.1 ml of 4:2:1 (by volume) water-chloroform-methanol mixture. Finally, the hydrophilic phase was removed, and the organic phase was saved and dried under a nitrogen gas stream.

Lipid profile characterization by thin-layer chromatography. The dried organic phase was resuspended with 4 μl of 2:1 (vol/vol) chloroform-methanol per 1 mg of dry weight. Fourteen microliters of each sample was applied on 60 F_{254} silica gel plates (Merck), and lipid components were separated by TLC using chloroform, methanol, ammonium hydroxide, and water (65:25:0.5:4) as a mobile phase. To develop plates, we repeated the process of pulverizing the staining solution and heating the plate at 100°C 4 to 5 times. To visualize the different glycolipids of the lipid mixture, we used α-naphthol staining, which contains 10.5 ml 15% ethanolic solution of 1-naphthol, 6.5 ml 97% sulfuric acid, 40.5 ml ethanol, and 4 ml water. Alternatively, total lipids were separated by 2D-TLC using chloroform, methanol, ammonium hydroxide, and water (65:25:0.5:4) as a mobile phase 1, and chloroform, acetic acid, methanol, and water (50:60:2.3:3) as mobile phase 2.

RNA extraction and quantitative reverse transcription-PCR. RNA extraction and quantitative reverse transcription-PCR were performed as previously described using the primers shown in Table S1 in the supplemental material (61). The *sigA* mRNA was used as internal invariant control for data normalization (36). RNA samples that had not been reverse transcribed were included in all experiments to exclude significant DNA contamination. For each sample, melting curves were performed to confirm the purity of the products.

Infection of macrophages. THP-1 macrophages (American Type Culture Collection) were grown in suspension at 37°C in 5% CO_2 in bicarbonate-buffered RPMI (Gibco) supplemented with 10% (vol/vol) fetal bovine serum (FBS; Gibco), 50 μmol/liter β-mercaptoethanol, and 50 μg/ml gentamicin to a density of about 0.5×10^6 cells/ml (34). To induce differentiation of monocytes into macrophages, cells were seeded in 96-well plates and stimulated with 50 ng/ml phorbol 12-myristate 13-acetate (PMA; Sigma-Aldrich). After 24 h, PMA was removed, and cells were infected with *M. tuberculosis* H37Rv and TB506.1 at a multiplicity of infection of 1:10 for 90 min as previously described (62). Extracellular bacteria were further removed by washing with warm phosphate-buffered saline (PBS), and fresh medium supplemented with 200 ng/ml ATc was added. Macrophages were lysed at 0 h and 2, 4, and 6 days after infection, and extracts were plated to determine viable bacteria.

Intranasal infection of mice. The mice used in the experiment were 7-week-old female C57BL/6J purchased from Envigo. Forty mice were challenged via the intranasal route with 10^3 CFU of *M. tuberculosis* H37Rv or TB506.1 suspended in 15 μl sterile PBS. For this procedure, mice were anesthetized with 75 mg/kg of ketamine and 1 mg/kg of medetomidine and reversed by 1 mg/kg of atipamezole. Drinking water was supplemented with 1 mg/ml of doxycycline (Sigma-Aldrich; D9891) and 5% sucrose. Control groups without doxycycline received drinking water with 5% sucrose. At day 1, week 4, and week 8 after infection, mice were euthanized in a CO_2 chamber, and lungs and spleen were collected for bacterial load estimation. The enumeration of viable CFU was performed by plating appropriate lung homogenate dilutions on Middlebrook 7H11 plates for *M. tuberculosis* H37Rv and Middlebrook 7H11 plates containing 50 μg/ml hygromycin and 20 μg/ml of streptomycin for TB506.1. The animal experiment was performed at the biosafety level 3 (BSL3) animal facilities of NEIKER Institute (Derio, Spain), having received institutional approval. All institutional and ethical guidelines for animal care and experimentation were adhered to with permits provided by "Diputacion Foral de Bizkaia 15/2017 and 20/2019." The NEIKER Animal Ethics Committee, registered with the Government of Spain (registration no. ES489010006099), approved all animal experimental protocols and usage.

Statistics. Statistical analyses were performed in GraphPad Prism 5.0. Two-way analysis of variance (ANOVA) with Tukey posttest was used to evaluate paired replicates. *P* values of less than 0.05 were considered significant.

SUPPLEMENTAL MATERIAL

Supplemental material is available online only.

SUPPLEMENTAL FILE 1, PDF file, 0.7 MB.

ACKNOWLEDGMENTS

This project was supported by grants from MINECO/FEDER EU contracts BFU2016-77427-C2-2-R, BFU2017-92223-EXP, PID2019-105649RB-I00; Severo Ochoa Excellence Accreditation SEV-2016-0644; the Basque Government contract KK-2019/00076; and NIH R01AI149297 (to M.E.G.). R.P.-R. is further a "Ramon y Cajal" fellow from the Spanish Ministry of Economy and Competitiveness. R.P.-R. acknowledges support by MINECO/FEDER EU contract SAF2016–77433-R and PID2019-110240RB-I00.

REFERENCES

1. Zumla A, Raviglione M, Hafner R, von Reyn CF. 2013. Tuberculosis. N Engl J Med 368:745–755. https://doi.org/10.1056/NEJMra1200894.
2. Guinn KM, Rubin EJ. 2017. Tuberculosis: just the FAQs. mBio 8:e01910-17. https://doi.org/10.1128/mBio.01910-17.
3. Getahun H, Matteelli A, Chaisson RE, Raviglione M. 2015. Latent Mycobacterium tuberculosis infection. N Engl J Med 372:2127–2135. https://doi.org/10.1056/NEJMra1405427.
4. World Health Organization. 2019. Global tuberculosis report 2019. World Health Organization, Geneva, Switzerland.
5. Horsburgh CR, Jr, Barry CE, III, Lange C. 2015. Treatment of tuberculosis. N Engl J Med 373:2149–2160. https://doi.org/10.1056/NEJMra1413919.
6. Dheda K, Gumbo T, Gandhi NR, Murray M, Theron G, Udwadia Z, Migliori GB, Warren R. 2014. Global control of tuberculosis: from extensively drug-resistant to untreatable tuberculosis. Lancet Respir Med 2:321–338. https://doi.org/10.1016/S2213-2600(14)70031-1.
7. Libardo MD, Boshoff HI, Barry CE, III. 2018. The present state of the tuberculosis drug development pipeline. Curr Opin Pharmacol 42:81–94. https://doi.org/10.1016/j.coph.2018.08.001.
8. Jackson M, McNeil MR, Brennan PJ. 2013. Progress in targeting cell envelope biogenesis in Mycobacterium tuberculosis. Future Microbiol 8:855–875. https://doi.org/10.2217/fmb.13.52.
9. Dulberger CL, Rubin EJ, Boutte CC. 2020. The mycobacterial cell envelope—a moving target. Nat Rev Microbiol 18:47–59. https://doi.org/10.1038/s41579-019-0273-7.
10. Johnson EO, LaVerriere E, Office E, Stanley M, Meyer E, Kawate T, Gomez JE, Audette RE, Bandyopadhyay N, Betancourt N, Delano K, Da Silva I, Davis J, Gallo C, Gardner M, Golas AJ, Guinn KM, Kennedy S, Korn R, McConnell JA, Moss CE, Murphy KC, Nietupski RM, Papavinasasundaram KG, Pinkham JT, Pino PA, Proulx MK, Ruecker N, Song N, Thompson M, Trujillo C, Wakabayashi S, Wallach JB, Watson C, Ioerger TR, Lander ES, Hubbard BK, Serrano-Wu MH, Ehrt S, Fitzgerald M, Rubin EJ, Sassetti CM, Schnappinger D, Hung DT. 2019. Large-scale chemical-genetics yields new M. tuberculosis inhibitor classes. Nature 571:72–78. https://doi.org/10.1038/s41586-019-1315-z.
11. Angala SK, Belardinelli JM, Huc-Claustre E, Wheat WH, Jackson M. 2014. The cell envelope glycoconjugates of Mycobacterium tuberculosis. Crit Rev Biochem Mol Biol 49:361–399. https://doi.org/10.3109/10409238.2014.925420.
12. Guerin ME, Kordulakova J, Alzari PM, Brennan PJ, Jackson M. 2010. Molecular basis of phosphatidyl-myo-inositol mannoside biosynthesis and regulation in mycobacteria. J Biol Chem 285:33577–33583. https://doi.org/10.1074/jbc.R110.168328.
13. Sancho-Vaello E, Albesa-Jove D, Rodrigo-Unzueta A, Guerin ME. 2017. Structural basis of phosphatidyl-myo-inositol mannosides biosynthesis in mycobacteria. Biochim Biophys Acta Mol Cell Biol Lipids 1862:1355–1367. https://doi.org/10.1016/j.bbalip.2016.11.002.
14. Khoo KH, Dell A, Morris HR, Brennan PJ, Chatterjee D. 1995. Structural definition of acylated phosphatidylinositol mannosides from Mycobacterium tuberculosis: definition of a common anchor for lipomannan and lipoarabinomannan. Glycobiology 5:117–127. https://doi.org/10.1093/glycob/5.1.117.
15. Jankute M, Cox JA, Harrison J, Besra GS. 2015. Assembly of the mycobacterial cell wall. Annu Rev Microbiol 69:405–423. https://doi.org/10.1146/annurev-micro-091014-104121.
16. Haites RE, Morita YS, McConville MJ, Billman-Jacobe H. 2005. Function of phosphatidylinositol in mycobacteria. J Biol Chem 280:10981–10987. https://doi.org/10.1074/jbc.M413443200.
17. Torrelles JB, Schlesinger LS. 2010. Diversity in Mycobacterium tuberculosis mannosylated cell wall determinants impacts adaptation to the host. Tuberculosis (Edinb) 90:84–93. https://doi.org/10.1016/j.tube.2010.02.003.
18. Morita YS, Fukuda T, Sena CB, Yamaryo-Botte Y, McConville MJ, Kinoshita T. 2011. Inositol lipid metabolism in mycobacteria: biosynthesis and regulatory mechanisms. Biochim Biophys Acta 1810:630–641. https://doi.org/10.1016/j.bbagen.2011.03.017.
19. Kordulakova J, Gilleron M, Mikusova K, Puzo G, Brennan PJ, Gicquel B, Jackson M. 2002. Definition of the first mannosylation step in phosphatidylinositol mannoside synthesis. PimA is essential for growth of mycobacteria. J Biol Chem 277:31335–31344. https://doi.org/10.1074/jbc.M204060200.
20. Guerin ME, Kaur D, Somashekar BS, Gibbs S, Gest P, Chatterjee D, Brennan PJ, Jackson M. 2009. New insights into the early steps of phosphatidylinositol mannoside biosynthesis in mycobacteria: PimB' is an essential enzyme of Mycobacterium smegmatis. J Biol Chem 284:25687–25696. https://doi.org/10.1074/jbc.M109.030593.
21. Lea-Smith DJ, Martin KL, Pyke JS, Tull D, McConville MJ, Coppel RL, Crellin PK. 2008. Analysis of a new mannosyltransferase required for the synthesis of phosphatidylinositol mannosides and lipoarbinomannan reveals two lipomannan pools in Corynebacterineae. J Biol Chem 283:6773–6782. https://doi.org/10.1074/jbc.M707139200.
22. Mishra AK, Batt S, Krumbach K, Eggeling L, Besra GS. 2009. Characterization of the Corynebacterium glutamicum ΔpimB' ΔmgtA double deletion mutant and the role of Mycobacterium tuberculosis orthologues Rv2188c and Rv0557 in glycolipid biosynthesis. J Bacteriol 191:4465–4472. https://doi.org/10.1128/JB.01729-08.
23. Torrelles JB, DesJardin LE, MacNeil J, Kaufman TM, Kutzbach B, Knaup R, McCarthy TR, Gurcha SS, Besra GS, Clegg S, Schlesinger LS. 2009. Inactivation of Mycobacterium tuberculosis mannosyltransferase pimB reduces the cell wall lipoarabinomannan and lipomannan content and increases the rate of bacterial-induced human macrophage cell death. Glycobiology 19:743–755. https://doi.org/10.1093/glycob/cwp042.
24. Brennan P, Ballou CE. 1967. Biosynthesis of mannophosphoinositides by Mycobacterium phlei. The family of dimannophosphoinositides. J Biol Chem 242:3046–3056. https://doi.org/10.1016/S0021-9258(18)95931-4.
25. Brennan P, Ballou CE. 1968. Biosynthesis of mannophosphoinositides by Mycobacterium phlei. Enzymatic acylation of the dimannophosphoinositides. J Biol Chem 243:2975–2984. https://doi.org/10.1016/S0021-9258(18)93368-5.
26. Kordulakova J, Gilleron M, Puzo G, Brennan PJ, Gicquel B, Mikusova K, Jackson M. 2003. Identification of the required acyltransferase step in the biosynthesis of the phosphatidylinositol mannosides of mycobacterium species. J Biol Chem 278:36285–36295. https://doi.org/10.1074/jbc.M303639200.
27. Guerin ME, Schaeffer F, Chaffotte A, Gest P, Giganti D, Kordulakova J, van der Woerd M, Jackson M, Alzari PM. 2009. Substrate-induced conformational changes in the essential peripheral membrane-associated mannosyltransferase PimA from mycobacteria: implications for catalysis. J Biol Chem 284:21613–21625. https://doi.org/10.1074/jbc.M109.003947.
28. Svetlikova Z, Barath P, Jackson M, Kordulakova J, Mikusova K. 2014. Purification and characterization of the acyltransferase involved in biosynthesis of the major mycobacterial cell envelope glycolipid—monoacylated phosphatidylinositol dimannoside. Protein Expr Purif 100:33–39. https://doi.org/10.1016/j.pep.2014.04.014.
29. Berg S, Kaur D, Jackson M, Brennan PJ. 2007. The glycosyltransferases of

Mycobacterium tuberculosis—roles in the synthesis of arabinogalactan, lipoarabinomannan, and other glycoconjugates. Glycobiology 17:35–56. https://doi.org/10.1093/glycob/cwm010.
30. Jackson M, Crick DC, Brennan PJ. 2000. Phosphatidylinositol is an essential phospholipid of mycobacteria. J Biol Chem 275:30092–30099. https://doi.org/10.1074/jbc.M004658200.
31. DeJesus MA, Gerrick ER, Xu W, Park SW, Long JE, Boutte CC, Rubin EJ, Schnappinger D, Ehrt S, Fortune SM, Sassetti CM, Ioerger TR. 2017. Comprehensive essentiality analysis of the Mycobacterium tuberculosis genome via saturating transposon mutagenesis. mBio 8:e02133-16. https://doi.org/10.1128/mBio.02133-16.
32. Albesa-Jove D, Svetlikova Z, Tersa M, Sancho-Vaello E, Carreras-Gonzalez A, Bonnet P, Arrasate P, Eguskiza A, Angala SK, Cifuente JO, Kordulakova J, Jackson M, Mikusova K, Guerin ME. 2016. Structural basis for selective recognition of acyl chains by the membrane-associated acyltransferase PatA. Nat Commun 7:10906. https://doi.org/10.1038/ncomms10906.
33. Tersa M, Raich L, Albesa-Jove D, Trastoy B, Prandi J, Gilleron M, Rovira C, Guerin ME. 2018. The molecular mechanism of substrate recognition and catalysis of the membrane acyltransferase PatA from mycobacteria. ACS Chem Biol 13:131–140. https://doi.org/10.1021/acschembio.7b00578.
34. Boldrin F, Ventura M, Degiacomi G, Ravishankar S, Sala C, Svetlikova Z, Ambady A, Dhar N, Kordulakova J, Zhang M, Serafini A, Vishwas KG, Vishwas VG, Kolly GS, Kumar N, Palù G, Guerin ME, Mikusova K, Cole ST, Manganelli R. 2014. The phosphatidyl-myo-inositol mannosyltransferase PimA is essential for Mycobacterium tuberculosis growth in vitro and in vivo. J Bacteriol 196:3441–3451. https://doi.org/10.1128/JB.01346-13.
35. Geiss F. 1987. Fundamentals of thin-layer chromatography (planar chromatography). Heidelberg, Basel, New York.
36. Manganelli R, Dubnau E, Tyagi S, Kramer FR, Smith I. 1999. Differential expression of 10 sigma factor genes in Mycobacterium tuberculosis. Mol Microbiol 31:715–724. https://doi.org/10.1046/j.1365-2958.1999.01212.x.
37. Sassetti CM, Boyd DH, Rubin EJ. 2003. Genes required for mycobacterial growth defined by high density mutagenesis. Mol Microbiol 48:77–84. https://doi.org/10.1046/j.1365-2958.2003.03425.x.
38. Griffin JE, Gawronski JD, Dejesus MA, Ioerger TR, Akerley BJ, Sassetti CM. 2011. High-resolution phenotypic profiling defines genes essential for mycobacterial growth and cholesterol catabolism. PLoS Pathog 7:e1002251. https://doi.org/10.1371/journal.ppat.1002251.
39. Boldrin F, Casonato S, Dainese E, Sala C, Dhar N, Palu G, Riccardi G, Cole ST, Manganelli R. 2010. Development of a repressible mycobacterial promoter system based on two transcriptional repressors. Nucleic Acids Res 38:e134. https://doi.org/10.1093/nar/gkq235.
40. Salman M, Lonsdale JT, Besra GS, Brennan PJ. 1999. Phosphatidylinositol synthesis in mycobacteria. Biochim Biophys Acta 1436:437–450. https://doi.org/10.1016/s0005-2760(98)00151-9.
41. Morii H, Ogawa M, Fukuda K, Taniguchi H, Koga Y. 2010. A revised biosynthetic pathway for phosphatidylinositol in Mycobacteria. J Biochem 148:593–602. https://doi.org/10.1093/jb/mvq093.
42. Morii H, Okauchi T, Nomiya H, Ogawa M, Fukuda K, Taniguchi H. 2013. Studies of inositol 1-phosphate analogues as inhibitors of the phosphatidylinositol phosphate synthase in mycobacteria. J Biochem 153:257–266. https://doi.org/10.1093/jb/mvs141.
43. Boldrin F, Degiacomi G, Serafini A, Kolly GS, Ventura M, Sala C, Provvedi R, Palu G, Cole ST, Manganelli R. 2018. Promoter mutagenesis for fine-tuning expression of essential genes in Mycobacterium tuberculosis. Microb Biotechnol 11:238–247. https://doi.org/10.1111/1751-7915.12875.
44. Taneja R, Malik U, Khuller GK. 1979. Effect of growth temperature on the lipid composition of Mycobacterium smegmatis ATCC 607. J Gen Microbiol 113:413–416. https://doi.org/10.1099/00221287-113-2-413.
45. Bansal-Mutalik R, Nikaido H. 2014. Mycobacterial outer membrane is a lipid bilayer and the inner membrane is unusually rich in diacyl phosphatidylinositol dimannosides. Proc Natl Acad Sci U S A 111:4958–4963. https://doi.org/10.1073/pnas.1403078111.
46. Morita YS, Patterson JH, Billman-Jacobe H, McConville MJ. 2004. Biosynthesis of mycobacterial phosphatidylinositol mannosides. Biochem J 378:589–597. https://doi.org/10.1042/BJ20031372.
47. Morita YS, Velasquez R, Taig E, Waller RF, Patterson JH, Tull D, Williams SJ, Billman-Jacobe H, McConville MJ. 2005. Compartmentalization of lipid biosynthesis in mycobacteria. J Biol Chem 280:21645–21652. https://doi.org/10.1074/jbc.M414181200.
48. Larrouy-Maumus G, Marino LB, Madduri AV, Ragan TJ, Hunt DM, Bassano L, Gutierrez MG, Moody DB, Pavan FR, de Carvalho LP. 2016. Cell-envelope remodeling as a determinant of phenotypic antibacterial tolerance in Mycobacterium tuberculosis. ACS Infect Dis 2:352–360. https://doi.org/10.1021/acsinfecdis.5b00148.
49. Matsumoto K. 1997. Phosphatidylserine synthase from bacteria. Biochim Biophys Acta 1348:214–227. https://doi.org/10.1016/s0005-2760(97)00110-0.
50. Evans JC, Trujillo C, Wang Z, Eoh H, Ehrt S, Schnappinger D, Boshoff HI, Rhee KY, Barry CE, III, Mizrahi V. 2016. Validation of CoaBC as a bactericidal target in the coenzyme A pathway of Mycobacterium tuberculosis. ACS Infect Dis 2:958–968. https://doi.org/10.1021/acsinfecdis.6b00150.
51. Guerin ME, Kordulakova J, Schaeffer F, Svetlikova Z, Buschiazzo A, Giganti D, Gicquel B, Mikusova K, Jackson M, Alzari PM. 2007. Molecular recognition and interfacial catalysis by the essential phosphatidylinositol mannosyltransferase PimA from mycobacteria. J Biol Chem 282:20705–20714. https://doi.org/10.1074/jbc.M702087200.
52. Giganti D, Albesa-Jove D, Urresti S, Rodrigo-Unzueta A, Martinez MA, Comino N, Barilone N, Bellinzoni M, Chenal A, Guerin ME, Alzari PM. 2015. Secondary structure reshuffling modulates glycosyltransferase function at the membrane. Nat Chem Biol 11:16–18. https://doi.org/10.1038/nchembio.1694.
53. Batt SM, Jabeen T, Mishra AK, Veerapen N, Krumbach K, Eggeling L, Besra GS, Futterer K. 2010. Acceptor substrate discrimination in phosphatidylmyo-inositol mannoside synthesis: structural and mutational analysis of mannosyltransferase Corynebacterium glutamicum PimB'. J Biol Chem 285:37741–37752. https://doi.org/10.1074/jbc.M110.165407.
54. Lairson LL, Henrissat B, Davies GJ, Withers SG. 2008. Glycosyltransferases: structures, functions, and mechanisms. Annu Rev Biochem 77:521–555. https://doi.org/10.1146/annurev.biochem.76.061005.092322.
55. Albesa-Jove D, Giganti D, Jackson M, Alzari PM, Guerin ME. 2014. Structure-function relationships of membrane-associated GT-B glycosyltransferases. Glycobiology 24:108–124. https://doi.org/10.1093/glycob/cwt101.
56. Albesa-Jove D, Guerin ME. 2016. The conformational plasticity of glycosyltransferases. Curr Opin Struct Biol 40:23–32. https://doi.org/10.1016/j.sbi.2016.07.007.
57. Moremen KW, Haltiwanger RS. 2019. Emerging structural insights into glycosyltransferase-mediated synthesis of glycans. Nat Chem Biol 15:853–864. https://doi.org/10.1038/s41589-019-0350-2.
58. Rodrigo-Unzueta A, Ghirardello M, Urresti S, Delso I, Giganti D, Anso I, Trastoy B, Comino N, Tersa M, D'Angelo C, Cifuente JO, Marina A, Liebau J, Mäler L, Chenal A, Albesa-Jové D, Merino P, Guerin ME. 2020. Dissecting the structural and chemical determinants of the "open-to-closed" motion in the mannosyltransferase PimA from mycobacteria. Biochemistry 59:2934–2945. https://doi.org/10.1021/acs.biochem.0c00376.
59. Giganti D, Alegre-Cebollada J, Urresti S, Albesa-Jove D, Rodrigo-Unzueta A, Comino N, Kachala M, Lopez-Fernandez S, Svergun DI, Fernandez JM, Guerin ME. 2013. Conformational plasticity of the essential membrane-associated mannosyltransferase PimA from mycobacteria. J Biol Chem 288:29797–29808. https://doi.org/10.1074/jbc.M113.462705.
60. Liebau J, Tersa M, Trastoy B, Patrick J, Rodrigo-Unzueta A, Corzana F, Sparrman T, Guerin ME, Mäler L. 2020. Unveiling the activation dynamics of a fold-switch bacterial glycosyltransferase by ^{19}F NMR. J Biol Chem 295:9868–9878. https://doi.org/10.1074/jbc.RA120.014162.
61. Maciąg A, Dainese E, Rodriguez GM, Milano A, Provvedi R, Pasca MR, Smith I, Palù G, Riccardi G, Manganelli R. 2007. Global analysis of the Mycobacterium tuberculosis Zur (FurB) regulon. J Bacteriol 189:730–740. https://doi.org/10.1128/JB.01190-06.
62. Manganelli R, Voskuil MI, Schoolnik GK, Smith I. 2001. The Mycobacterium tuberculosis ECF sigma factor σ^E: role in global gene expression and survival in macrophages. Mol Microbiol 41:423–437. https://doi.org/10.1046/j.1365-2958.2001.02525.x.